REPORT DOCUMENTATION PAGE

Form Approved
OMB NO. 0704-0188

1. AGENCY USE ONLY (Leave Blank)	2. REPORT DATE	3. REPORT TYPE AND DATES COVERED
	06/16/03	Final **07/01/00-01/31/03**

4. TITLE AND SUBTITLE
Parallel, Ultrafast Sub-100 Nanometer Dip-Pen Nanolithography

5. FUNDING NUMBERS
DAAD19-00-1-0414

6. AUTHOR(S)
Dr. Chad A. Mirkin, Northwestern University, Evanston IL
Dr. Chang Liu, University of Illinois, Urbana-Champaign

7. PERFORMING ORGANIZATION NAME(S) AND ADDRESS(ES)
NU, Department of Chemistry, 2145 Sheridan Rd., Evanston, IL 60208-3113
U of I, Microelectronics Laboratory, Champaign, IL 61801

8. PERFORMING ORGANIZATION REPORT NUMBER
#1-2000

9. SPONSORING / MONITORING AGENCY NAME(S) AND ADDRESS(ES)

U. S. Army Research Office
P.O. Box 12211
Research Triangle Park, NC 27709-2211

10. SPONSORING / MONITORING AGENCY REPORT NUMBER

41503.1-PH

11. SUPPLEMENTARY NOTES
The views, opinions and/or findings contained in this report are those of the author(s) and should not be construed as an official Department of the Army position, policy or decision, unless so designated by other documentation.

12 a. DISTRIBUTION / AVAILABILITY STATEMENT

Approved for public release; distribution unlimited.

12 b. DISTRIBUTION CODE

20030925 024

13. ABSTRACT (Maximum 200 words)

We have developed new designs and fabrication techniques for arrayed (one dimensional and two dimensional) DPN probes in two categories, passive probes and active probes. We have successfully developed mechanical and electrical interfaces to commercial AFM machines and software. Arrayed DPN writing has been achieved. As a highlight, a set of ten different characters has been written using ten different pens in one single run. We also have significantly advanced the chemistry compatible with the DPN technique. We have demonstrated the patterning of organic molecules (e.g., self-assembled monolayers) biological molecules (protein, and DNA molecules) and inorganic materials (e.g., sol-gel, silicon, and magnetic nanoparticles). Potential applications of DPN have now been extended to the semiconductor industry (e.g., mask repair and patterning of semiconductor substrates and thin films with sub-100 nm resolution), as well as military and medical diagnostics (e.g., DNA and protein arrays). We also have developed efficient and high yield microfabrication processes for realizing 2D probe arrays with uniform and small tip radii. A method for detecting tip/substrate contact has been developed using electrical continuity.

In summary, we have successfully completed proposed tasks outlined in the proposal. We plan to develop high-density 2D array DPN probes with efficient inking method.

14. SUBJECT TERMS
Dip Pen Nanolithography, DPN, microfabrication, active probe array, passive probe array

15. NUMBER OF PAGES
32

16. PRICE CODE

17. SECURITY CLASSIFICATION OR REPORT	18. SECURITY CLASSIFICATION ON THIS PAGE	19. SECURITY CLASSIFICATION OF ABSTRACT	20. LIMITATION OF ABSTRACT
UNCLASSIFIED	**UNCLASSIFIED**	**UNCLASSIFIED**	**UL**

NSN 7540-01-280-5500

Standard Form 298 (Rev.2-89)
Prescribed by ANSI Std. 239-18

298-102

Parallel, Ultrafast Sub-100 Nanometer Dip-Pen Nanolithography

Chad Mirkin
Institute for Nanotechnology, Northwestern University

Chang Liu
Micro and Nanotechnology Laboratory, University of Illinois

A. Statement of the problem studied

ABSTRACT

Over the past three years, significant progress has been made in two general areas: (1) development of parallel and active DPN probes for high throughput DPN writing; (2) characterization of the DPN transfer process and development of means to functionalize and process metal and semiconductor substrates. Specific research activities are summarized under these two major areas.

Area 1: Development of parallel and active DPN probes for high throughput DPN writing.

1.1. We have fully developed a thermal-bimetallic actuated, active, and parallel DPN probe. Two probes, made of silicon and of silicon nitride, have been made.
1.2. We also have built comprehensive thermal transfer and mechanical deformation models to optimize the design of such probe arrays.
1.3. We have developed a custom mechanical DPN chip holder with multiple degrees of freedom including two rotational DOF. The holder is mounted on a commercial scanning-probe microscope.
1.4. We have developed a method for controlling the movement of multiple probes as well as to compensate for thermal cross-talk among neighboring probes.
1.5. We have successfully performed parallel DPN writing experiments. A method for coating ODT inks onto arrayed DPN probes has been developed.
1.6. We have successfully developed a new method for detecting contact between a DPN tip and a conductive writing surface without relying on the use of laser beam reflection.
1.7. We have developed a new method for forming through-wafer microfluidic interconnects. The application of such interconnects is to enable arrayed ink delivery.
1.8. We have developed DPN probes based on low cost polymer materials and a companion fabrication process.

Area 2: Characterization of the DPN transfer process and development of a means to functionalize and process metal and semiconductor substrates.

2.1. We have comprehensively characterized the DPN writing performance as a function of the relative humidity, for MHA and ODT inks. The results of this study were published in the *Journal of Physical Chemistry B*.
2.2. We have developed and published DPN techniques for generating sub-50 nm metal (*Nano Letters, Advanced Materials*), insulating thin films (*Journal of the American Chemical Society*), and magnetic structures (*Advanced Materials*).
2.3. We have developed a method for directly transferring oligonucleotide molecules onto substrates. A paper on this topic was published in the journal *Science*.
2.4. We have developed a method for transferring protein molecules onto a substrate. Papers on this topic were published in the journals *Science*, *Angewandte Chemie*, and *the Journal of the American Chemical Society*.
2.5. We have developed a new method for reducing the width of DPN writing traces using an electrical whittling method (published in *Nano Letters*).

B. Summary of the most important results

1. Detailed Report

Area 1.1: We have fully developed a thermal-bimetallic actuated, active, and parallel DPN probe. Two probes, made of silicon and of silicon nitride, have been made.

The fabrication process used to produce TA-DPN probes is shown in Figure 1. (a) The process begins with an oxidized <100> wafer. (b) The oxide is patterned into squares that act as a mask against an anisotropic wet etch to form silicon pyramids. (c) The apex of the pyramids are sharpened by several repetitions of thermal oxidation and oxide removal. (d) Silicon nitride is then deposited by LPCVD and patterned with Freon-14 RIE to form the beams. (e) Chromium and gold are then deposited and patterned to form the metal heater leads and actuator. (f) Finally, the beam is released by a second anisotropic wet etch from the front side of the wafer.

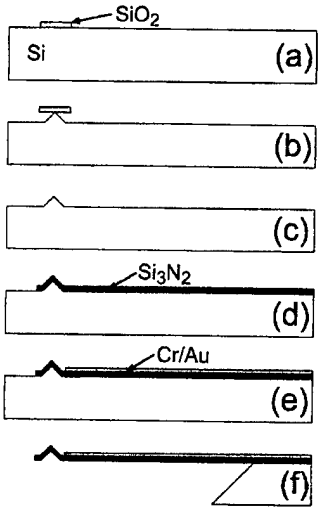

Figure 1: Schematic diagram of microfabrication process.

The silicon nitride film was characterized using three sequential tests that are described here in the order performed. The modulus of elasticity was found first using nanoindentation. The measurement was obtained with a Hysitron TriboScope® installed on a DI Multimode AFM. A Berkovitch diamond indenter was used, resulting in a value of E_{Si3N4}=224.6 GPa. This value is near the low end of published values for similar processes.

The coefficient of thermal expansion (CTE) of silicon nitride was estimated using two 50μm x 250μm test bimetallic beams mounted on TA-DPN probe chip. The beams are composed of the same films used in the actual devices but have no heaters and lack any complex geometry in order to minimize the effects of local stress variations near film boundaries. The beams were heated in a thermal bath to guarantee a uniform temperature distribution and the resulting tip deflection was compared with the analytical model. Under these conditions, the silicon nitride CTE is the only fitting parameter in the model and the best fit was found at $\alpha_{T,Si3N4}=0.3x10^{-6}$ °C^{-1}. A relatively low value is expected in light of the high elastic modulus and film density that results from the LPCVD deposition process. When this value is used to model actual TA-DPN probes at uniform temperature, the estimated tip deflection is within 10% of the actual deflection at all temperatures ranging from 0 to 50°C above ambient.

The thermal conductivity was found in the third test by operating a TA-DPN probe in a vacuum (<300mT). Vacuum operation drastically reduces convection heat transfer and results in a thermal profile that is dominated by heat conduction to the substrate (the low temperature differences with the environment allow radiation to be ignored). Again, the tip deflection results were compared with the analytical model at various heater current values. Under these conditions, the thermal conductivity of silicon nitride is the only fitting parameter and the best fit was found at k_{Si3N4}=1.7W/mK, which is within the range of published thin film values.

The final value required for complete evaluation of the thermal model is the apparent convection heat transfer coefficient. During optimization, this value must be estimated since Nusselt number correlations are not available for free convection at this scale. After device fabrication, it can be experimentally determined by fitting the analytical model to the experimentally calculated data from a TA-DPN probe operating in air. Under these conditions, the convection coefficient is the only fitting parameter and the best fit was found at h=700W/m^{2}K. As indicated by (2), this is the apparent convection coefficient based on the assumption that the same value is applied to all surfaces of the probe. The large value suggests that heat transfer between the beam and the environment is probably dominated by conduction through the air to adjacent probes and the holder chip. This presents a unique modeling challenge that is currently under investigation. The table below shows a comparison between experimental and analytical results for the probe operation in air and a vacuum.

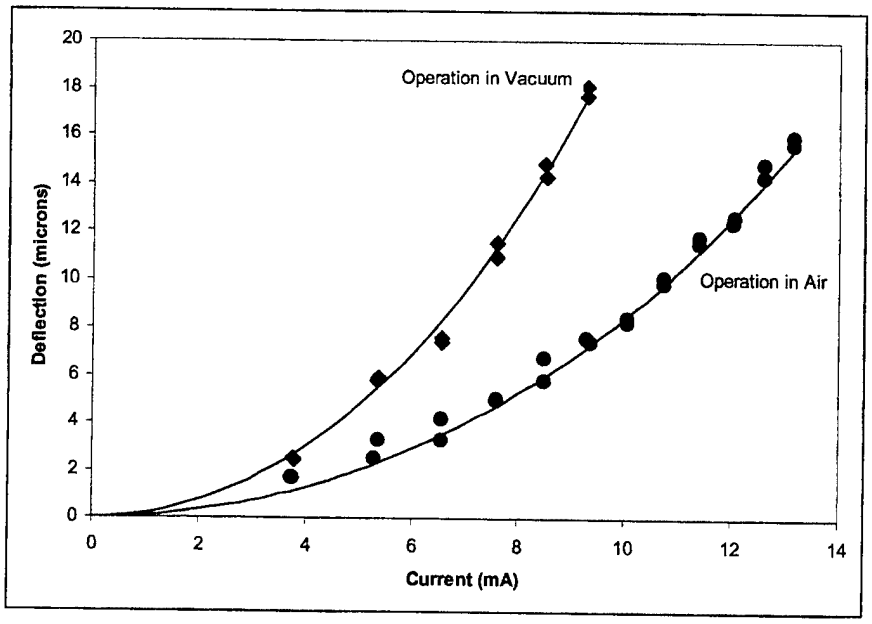

Figure 2: Theoretical prediction and measured deflection as a function of input current.

To demonstrate the independent pattern generation capability of this device, the 10 probes were used to simultaneously write the numerals 0-9 (Figure 3). After coating and installation in the AFM, the array was aligned with the gold substrate and then passed through a figure-8 pattern.

The figure-8 pattern was 6μm tall, 4μm wide, and was traversed in 8 steps at 1μm/sec (except step 7 which was traversed at 20μm/sec). A different numeral was written with each probe by selectively actuating the probe to lift its tip off the surface and suspend deposition.

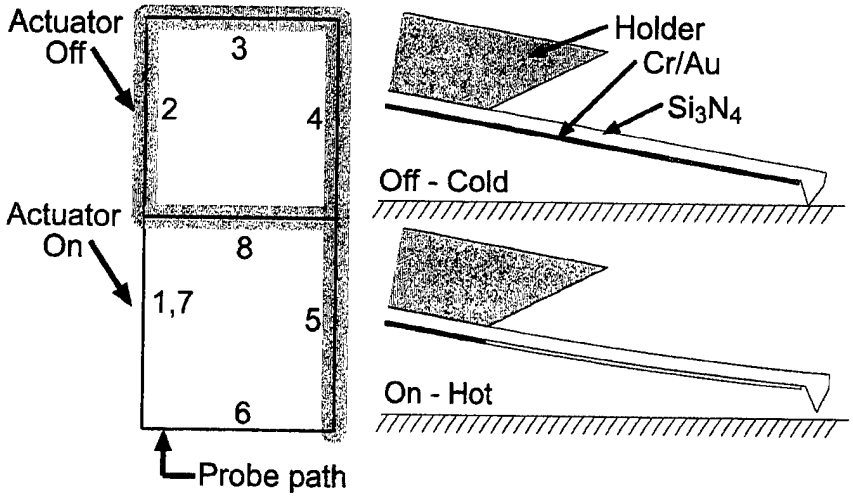

Figure 3: Different numerals are generated from a common figure-8 pattern using thermal actuation. Actuated probes are hot and lift from the surface to suspend lithography. Cold probes are on the surface and perform deposition.

After deposition, the patterns were imaged with lateral force microscopy (LFM) using a commercial silicon nitride contact mode AFM probe. ODT forms a self-assembled monolayer with lower surface friction than the bare gold, thus showing up as a dark region. A typical set of patterns is shown in Figure 4. This image shows each of the ten patterns written simultaneously by the ten TA-DPN probes. The patterns exhibit a narrow line surrounded by a dim halo. The inner line most likely represents the solid-solid contact between probe and surface and has an average width of 150nm. The halo is larger than the meniscus that forms between the tip and substrate and most likely forms by the ODT diffusion from the contact point after deposition. Its size is sensitive to many tip and surface variables and its cause and remediation are under investigation by several groups. The number '3', '4', and '9' patterns show a faint line that was drawn during step 7 of the probe traverse. It results from a slight timing error between translation and actuation and is being addressed in the latest version of the system.

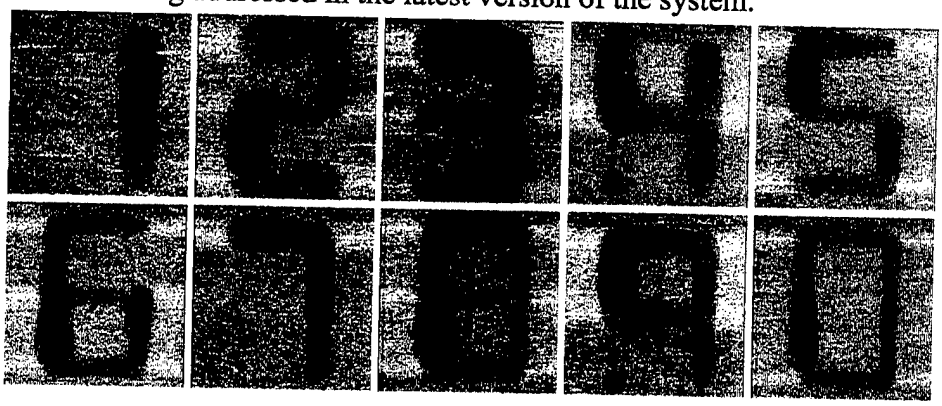

Figure 4: Typical DPN patterns from multi pen writing. Each LFM scan is 8mm x 8mm.

Area 1.2: We have built comprehensive thermal transfer and mechanical deformation models to optimize the design of such probe arrays.

The layout of a TA-DPN probe array is illustrated in Figure 5. The design consists of a silicon probe chip with a 1-D array of rectangular cantilever probes at one end. Each probe is made of silicon nitride with a pyramidal tip at its apex. A gold layer on the tip side of the silicon nitride cantilever creates the bimetallic actuator. The gold is patterned into a thin wire located at the base of the probe. This acts as an ohmic heater and an actuation patch over the remaining length. The films are stacked such that the tip moves away from the surface when heated. The dimensions, fabrication, and operation will be discussed later.

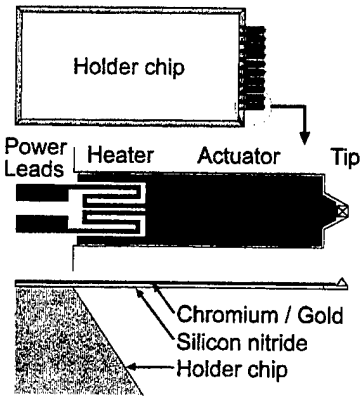

Figure 5: General layout of a TA-DPN probe array. Each probe chip has 10 thermally actuated probes at one end. Each probe consists of a Si_3N_4 cantilever with a gold layer that is patterned to form a heater and actuator.

DPN probes do not require feedback control of the tip height during any portion of their operation. This simplifies the device design, minimizes hardware support requirements, and yields an inexpensive scanning probe lithography system. It also means that there is no way to actively adjust the tip-substrate contact condition to accommodate changing conditions. Thus the design must be carefully crafted to avoid potential failure modes. The actuators must be strong enough to overcome surface adhesion, soft enough to prevent surface scratching, and provide enough deflection to overcome array-to-substrate misalignment without excessive operating temperatures.

To design and optimize devices within these constraints, a compact analytical macro-model has been created. The model consists of a thermal model of the cantilever and a film stress induced beam-bending model. Both are analytical in nature and general enough to evaluate cantilevers with an arbitrary layout. The two models are uncoupled and solved sequentially.

The thermal model is based on the assumption of 1-D heat diffusion along the probe length. Although somewhat restrictive, this assumption allows a rapid solution (essential for device optimization) and becomes more valid as beam length/width and length/thickness ratio increases. Convective cooling is assumed to be present on all surfaces and fully characterized by a single, constant, convection heat transfer coefficient. The probe base is assumed to remain at a fixed temperature equal to the substrate temperature (verified by finite element analysis of the substrate). The thermal conductivity of all materials is assumed constant but the heat supplied by the resistive heater is a function of temperature due the large temperature coefficient of resistance of the heater material.

The thermal problem is setup by first dividing the probe along its length into thermally distinct sections. Within each section, the layer materials and cross sectional geometry are constant over the section length. Thus the same heat diffusion equation is valid over the entire section length. As shown in Figure 1b, changes in layer geometry can be used to divide the probe presented in this paper into 8 different sections. Three constants are defined for each section. The total area-thermal conductivity product is given by

$$K = \sum_{i=1}^{n} k_i w_i t_i \tag{1}$$

where k, w, and t are the thermal conductivity, width, and thickness of each, material layer i in the cross section with n total layers. The convection-perimeter product is given by

$$H = 2h\left(W + \sum_{i=1}^{n} t_i\right) \tag{2}$$

where h is the effective, temperature-invariant, surface-invariant convection coefficient and W is the width of the widest layer. The heat generation is temperature dependant because the heater resistance is a function of temperature as given by $R=R_o\,[1+\alpha_r(T- T_o)]$ (where R_o is the total resistance of the serpentine heater at a reference temperature T_o and α_r is the temperature coefficient of resistivity of the heater material). The temperature-invariant component of the heat generation per unit length is given by

$$P = N\left(I^2 R_o / L\right) \tag{3}$$

where L is the total length of the heater wire, I is the constant applied heater current, and N is the number of passes the heater lead makes through the section (for example, in section 3 of the beam shown in Figure 1b, the heater lead makes 6 passes through the third section).

In terms of these three constants, the steady state heat diffusion equation (HDE) is found to have the form

$$\frac{\partial^2 T}{\partial x^2} - \left(\frac{H - P\alpha_r}{K}\right) T = -\frac{HT_\infty + P\left(1 - \alpha_r T_o\right)}{K}. \tag{4}$$

The solution to (4) is analytical and has one of two forms depending on the sign of $(H-P\alpha_r)$. With exception of the tip section, the boundary conditions at both ends of each section are fixed temperature. The tip section has a constant temperature condition at one end and a convection condition at the other. To find the temperature profile of the entire beam, this system of ODE's with their coupled temperature boundary conditions is solved simultaneously.

Once the temperature profile is known, it can be used to find the deflection profile. This is done by discritizing the probe along its length and using the local average temperature to find the local radius of curvature resulting from thermal stress. The deflection profile then found geometrically. The local radius of curvature is found by first finding the location of the neutral axis as given by

$$\bar{y} = \frac{\sum_{i=1}^{n} E_i w_i t_i \left(t_i/2 + \sum_{j=1}^{i-1} t_j\right)}{\sum_{i=1}^{n} E_i w_i t_i}, \tag{5}$$

where E_i is the biaxial modulus. The outer summation (i) is applied over all layers while the inner summation (j) is over the layers below layer i. The term in parenthesis is the distance from the bottom of the beam to the middle of the ith layer. The flexural stiffness of the beam is given by

$$I_{eff}E_o = \sum_{i=1}^{n}\left[\frac{E_i w_i t_i^3}{12} + E_i w_i t_i\left(\left(\frac{t_i}{2} + \sum_{j=1}^{i-1} t_j\right) - \bar{y}\right)^2\right], \tag{6}$$

where E_o is an arbitrary reference modulus. Summing the moments exerted on the beam by each layer gives the total moment due to thermal stresses

$$M = \sum_{i=1}^{n}\left[E_i w_i t_i\left(\frac{\sum_{i=1}^{n} E_i w_i t_i \alpha_{T,i}\Delta T}{\sum_{i=1}^{n} E_i w_i t_i} - \alpha_{T,i}\Delta T\right)\left(\frac{t_i}{2} + \sum_{j=1}^{i-1} t_j\right)\right] \tag{7}$$

where α_T is the thermal expansion coefficient and ΔT is the difference in temperature between the reference temperature and the operating temperature as found from the probe temperature solution (typically $\Delta T = T - T_\infty$). The resulting radius of curvature is given by

$$R = \frac{I_{eff}E_o}{M}. \tag{8}$$

Since (8) is evaluated at each location along the probe length, temperature dependant mechanical properties can be evaluated if they are known (they were not used in our simulations). In addition, the stress terms in (7) can be expanded to include other sources of film stress such as deposition stress, piezoelectric stress, and stress gradients to create a more comprehensive model.

When limited by a maximum allowable operating temperature, thermally actuated DPN probe arrays have essentially four primary failure modes. They may fail to generate enough force to overcome surface adhesion. They may not develop enough deflection to overcome array-to surface misalignment or surface topological features. They may scratch the substrate when pressed down to overcome array-to surface misalignment and, finally, thin film stresses may deform the released probes into unusable shapes. Optimization within these constraints may be done with finite element methods but this is not the optimal solution. Evaluating these failure modes means evaluating the probe, the tip-to-substrate contact, and the fluid meniscus. Setting up and solving such a multi-physics problem using finite elements is very time consuming.

To obtain a fast first-order analysis of potential designs, the optimization routine used here relies entirely on analytical analysis. It has been previously described and is only briefly reviewed here. In this method, the probe force, deflection, and shape are evaluated the model described above. The tip-to-substrate mechanics are evaluated using Hertzian contact mechanics and the meniscus is evaluated using thermodynamic methods.

To optimize the probe design, a large block of potential layouts is selected based on the thickness of the constituent films and overall length of the probe. Each design is evaluated based on the failure criteria and successful designs are plotted against the film thickness and probe length. The result is a 3-D plot of the designs that, to a first order approximation, meet all the important criteria. Depending on the coding of the simulation and the hardware used, 10's or 100's of thousands of designs can be examined in a matter of hours by testing large blocks of designs and plotting the successful and failing ones, the relationships between them can be readily understood (Figure 6). The benefit of this understanding should not be underestimated when dealing with complex and conflicting constraints.

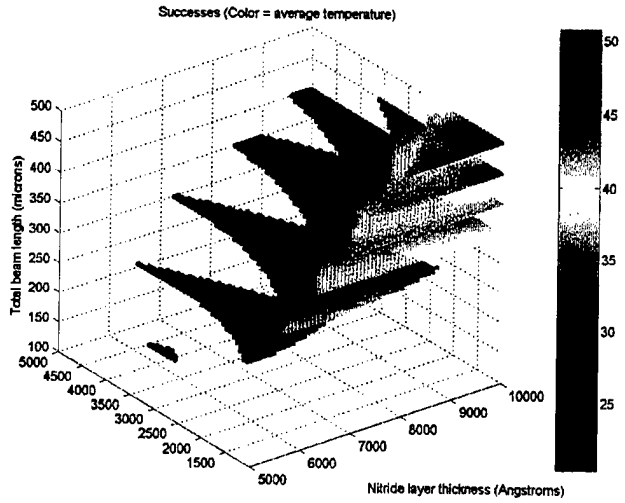

Figure 6: Successful TA-DPN probe array designs based on an analysis of 33,000 potential designs. 14.8% were successful and are plotted. The graph color represents the average operating temperature of each probe.

The final TA-DPN probe layout was found using the simulation/optimization methods described above along with data collected from test devices structures that were used to identify material properties. The optimization was focused on creating a 10-probe array for use writing 1-octadecanethiol (ODT) patterns on a gold surface. ODT was chosen because it can be coated onto the probe surface from the vapor phase and easily withstands temperatures up to 65°C without degradation. A gold substrate was chosen since the ODT/AU system is well characterized and many DPN applications use thiol-modified chemicals on gold surfaces. The minimum achievable array-surface angular misalignment was estimated at 0.2 degrees based on hardware limitations. Adhesion force was estimated from a worst-case scenario that involved complete inundation of the spherical region of the tip by the meniscus.

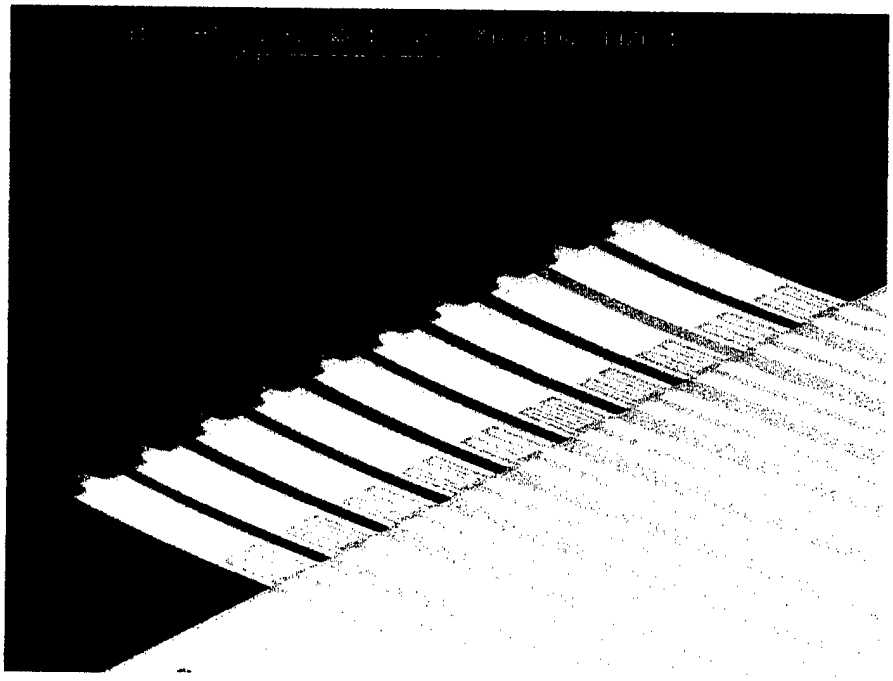

Figure 7: An array of TA-DPN probes.

The combination of fabrication limitations, AFM limitations, and direct and indirect limitations imposed by the above criteria lead to the optimal design show in Figure 7. Each probe is 300μm long (295 from probe base to tip apex), 80μm wide, and made of 9650Å thick silicon nitride and 3650Å thick gold with a 250Å thick chromium adhesion layer. The serpentine gold wire at the base acts as the ohmic heater while the remaining gold acts with the silicon nitride beam as a bimetallic thermal actuator. The probe tips are approximately 5μm tall and heating the beam causes them to lift away from the surface. The radius of curvature of the tip is approximately 9000Å. Each probe array consists of 10 individual probes on a single 1.5mm x 2.2mm silicon chip. The wire traces are arranged to provide a single power lead for each probe and a common ground without overlapping traces. Tip-to-tip spacing is 100μm, resulting in a 20μm gap between individual probes.

Area 1.3: We have developed a custom mechanical DPN chip holder with multiple degrees of freedom DOF including two rotational DOF. The holder is mounted on a commercial scanning-probe microscope.

The probe array design shown in Figure 7 has been demonstrated in DPN patterning applications. Since commercial AFM's are not compatible with multiprobe arrays, a Thermomicroscopes M5 AFM was modified for this demonstration. The modification consisted of the addition of a mechanical tip-tilt stage to the scan head of the AFM. The stage allows the probe array to be rotated from front to back about a line passing through all the tips (±20° with a resolution of ~0.1°), and side to side (+18°/-14° with the same resolution). The probe chip is mounted on a holder that allows it to be connected to an external control circuit. A photograph of the assembled device system is shown in Figure 8. A video microscope provides a side view of the array and augments the M5's overhead view during array-sample alignment.

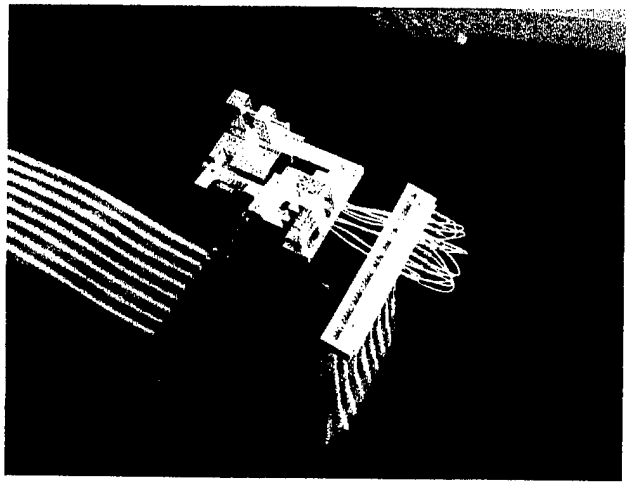

Figure 8: Test setup installed on the scan head of the M5.

Area 1.5: We have successfully performed parallel DPN writing experiments. A method for coating ODT inks onto arrayed DPN probes has been developed.

In preparation for use, the probe arrays are coated with 1-octadecanethiol (ODT). The probes are first stripped of organic contaminants with a 30 second oxygen plasma etch. They are then coated by vaporizing ODT from a molten source at 60°C and allowing the vapor to condense on the probe surfaces at room temperature for approximately 30min. After coating, the probes are installed and the total resistance of each actuator circuit is normalized to 500Ω with a series variable resistor.
To create a smooth lithography surface, the substrate is prepared from a polished <100> silicon wafer. The wafer is stripped of oxide in buffered HF, diced into small chips (approx. 3mm x 5mm), cleaned with acetone/isoproponal/water, and dried on a hotplate at 270°C for 5min. A 5nm chromium and 20nm gold thin film are then deposited by thermal evaporation. The samples are stored in ambient air until use (typically between 1 and 48 hours). During all lithography experiments, the ambient environment is held at 26°C and 52-55% relative humidity.

Area 1.6: We have successfully developed a new method for detecting contact between a DPN tip and a conductive writing surface without relying on the use of a laser beam.

In order to implement parallel DPN processes, it is essential that the tips of all the probes in an array contact the writing surface simultaneously. The alignment is a challenging task due to small tolerances and large, high- density arrays. It is critical that the contact state between the probes and the writing surface be monitored in real time simultaneously. Current SPM instruments utilize a single laser beam to monitor the contact between a single scanning tip and the writing surface of interest. However, it would be tedious and prohibitively difficult to use the single laser to detect the contact states of multiple probes at once. Ideally, the contact sensing method should involve simple fabrication and little modification to commercial SPM probes, provide high sensitivity, and be easy and inexpensive to implement.

In this paper, a new contact sensing method is proposed and experimentally investigated. It is based on the detection of electrical continuity between a scanning tip and a writing surface (Figure 9). It is conjectured that the electrical resistance between the probe tip (Terminal A) and the writing surface (Terminal B) serve as a sensitive indicator of physical contact. This method requires that both the scanning probe and the writing surface be partially or entirely conductive. In case the scanning probes are made of non-conductive materials, they can be coated with metal thin films, with metal conducting traces running from the tip to the handle. If the writing surface is non-conductive, this method is still useful if electrically connected islands of conductive films can be formed on the writing surface.

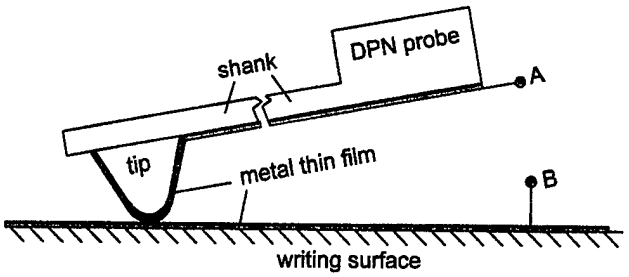

Figure 9: Schematic diagram of conductivity-based contact sensing method.

We first fabricated DPN probe arrays made of silicon nitride and coated them with a thin gold film. We then utilized these probes to conduct a series of experiments to investigate this new contact sensing method. These tests are summarized below:

(1) We characterized the electrical resistance as a function of the distance between the probes and the sample surface. In this test, the tip surface was not coated with ink adsorpants.

(2) We coated the probes with 1-octadecanethiol (ODT), a common DPN ink, and repeated the first experiment. This test is necessary because contact-sensing probes might be coated with chemicals accidentally or intentionally. This test would establish the effect of ODT on the electrical characteristics.

(3) We demonstrated that parallel DPN writing with multiple probes could be successfully performed using the contact sensing method proposed in this paper.

The contact sensing probe was mounted on the XYZ scan head and driven to within several micrometers above the sample surface (Figure 10). After that, the gap between the probe and the sample surface was carefully adjusted using the piezoelectric scanning tube with moving speed of approximately 30 nm/sec. A CCD microscope was used to visually observe the movement of the probe. It should be noted that the camera couldn't provide sufficient resolution and field of view to discern actual tip contact events.

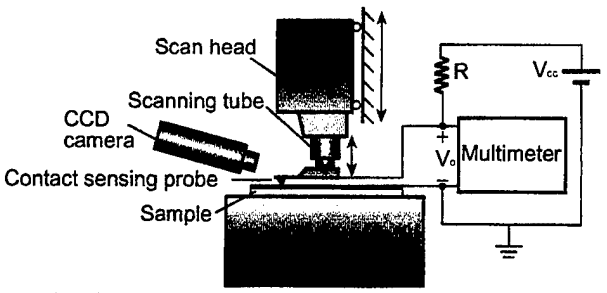

Figure 10: Schematic of the contact sensing test setup.

In our experiments, a DC bias voltage (V_{cc}) was applied between the probe and the sample surface. A 15 MΩ series resistor (R) was used to limit the current density at the contact point. The voltage drop between the probe and the sample surface (V_o) was measured using a HP 34401A multimeter, which has an input impedance of 10MΩ. In this case, V_o equals to 40% of V_{cc} when the contact is open and drops to almost 0V when a contact is made. We monitored the change in the contact resistance by measuring the voltage drop between the probe tip and the sample surface.

Figure 11 shows SEM micrographs of an array of ten probes for contact sensing experiments. Each probe is composed of a cantilever beam made of silicon nitride and a thin-film metal wire lead (200-nm-thick gold). The fabrication process has been discussed in the past. The length, width and thickness of each probe shank are 300μm, 80μm and 1.25μm (total), respectively. The distance between neighboring tips is 100 μm. The radius of curvature of the tips is approximately 1200 nm. The effective force constant of the composite probe was analytically estimated to be approximately 0.17N/m. The sample was a 250-μm-thick silicon wafer coated with 30nm-thick evaporated gold film.

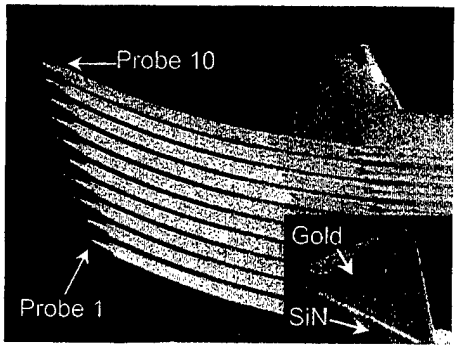

Figure 11: Scanning electron micrographs of the silicon-nitride probes and an individual tip.

In the first experiment, we measured the voltage drop (V_o) as a function of distance. The output characteristics of each probe in the array were tested separately and the testing was repeated ten times for each probe. Before the testing, V_o was set to 62.5 mV. We found that (1) the contact-sensing test could be repeated many times for each probe, indicating the contact metal was not damaged at contact; (2) the signal/noise ratio was high enough to clearly indicate the contact event. The bias voltage V_o may be further optimized or lowered. However, this is beyond the scope of this paper.

Figure 12 shows the testing result of a representative probe, Probe 1. As the tip approaches the sample surface, V_o drops from 62.5mV to 0V within a distance of 15nm. This drop in voltage corresponds to the electrical grounding of the tip due to physical contact with the sample surface. This contact sensing method has a sensitivity of at least 15 nm, which is adequate for DPN applications. As the tip is withdrawn from the sample surface, the voltage output rises from 0 back to 62.5 mV at a different displacement value. This hysteresis is affected by the magnitude of the tip-surface adhesive forces, the cantilever compliance, and the tip sharpness. However, the investigation of the hysteresis is not a major concern at this stage since only the transition occurring during the tip approach (not withdraw) is critical to the alignment process.

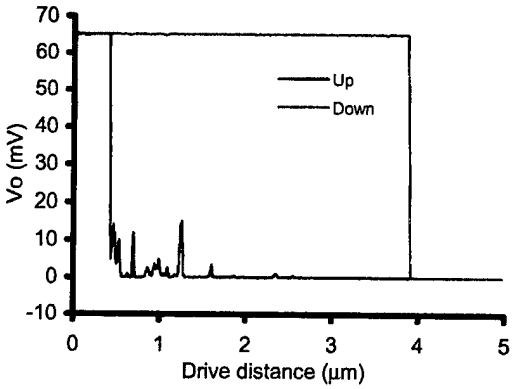

Figure 12: Contact sensing testing result of Probe 1.

Next, the second experiment was conducted to determine electrical contact characteristics in the presence of ODT, a very common material used for DPN. Before testing, all of the probes were thoroughly cleaned using oxygen plasma and then vapor-coated with ODT for 1 h. Figure 13 shows the testing result of Probe 1. We found that if the bias is lower than a certain threshold value (corresponding to V_o<3V), the output remains constant even when the probe was fully in contact with the sample surface (based on visual inspection). However, if the bias is initially set higher than the threshold voltage, V_o changes in the same way as in the first experiment. Figure 13 also shows that the cycle hysteresis became smaller when the probes were coated with ODT. We believe that this is due to reduced surface adhesion at the presence of ODT.

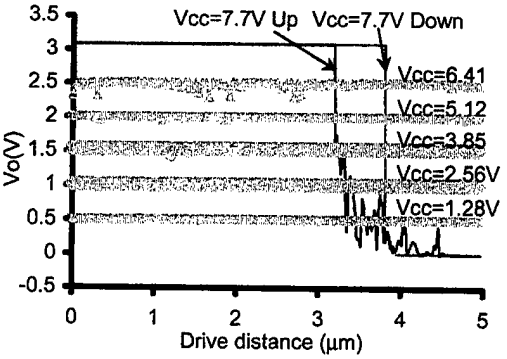

Figure 13: Contact testing result of Probe 1 with ODT coating.

The threshold voltage was further characterized using a semiconductor I-V curve tracer (Figure 14). The probes were cleaned with oxygen plasma and re-coated with

ODT using the same procedure. We mechanically pressed a probe into full contact with the sample surface under zero bias voltage (V_{cc}). We gradually increased the bias voltage while recording the voltage drop (V_o) simultaneously. As is shown in Figure 14, V_o first increases linearly with V_{cc}, which shows that although the probe is in contact with the sample surface, it is still electrically isolated from the writing sample by the ODT film. However, when V_{cc} is increased to 6.8V, V_o begins to drop until it becomes almost zero when V_{cc} reaches 7.6V. This indicates that the ODT coating has a breakdown voltage of about 2.96V, which matches the result obtained in the previous test.

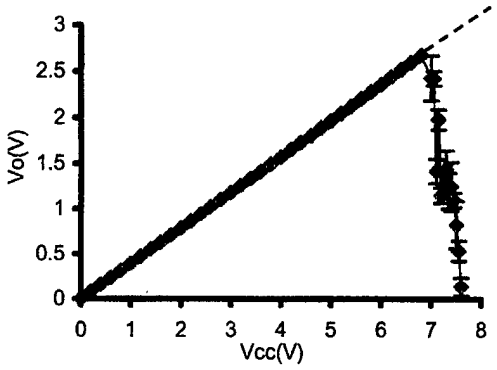

Figure 14: Breakdown testing of ODT coating on Probe 1.

The application of the new contact sensing method in DPN applications was demonstrated using a one-dimensional silicon nitride probe array similar to the one shown in Figure 11, except that only Probe 1, 5, 6 and 10 have patterned metal leads. The probes on the extreme ends of the array, Probe 1 and 10, served as contact sensors, while the remaining eight probes were used for DPN writing. The writing surface is a 30nm-thick gold film on a silicon substrate.

The probe array was vapor-coated with ODT using the same procedure. A bias voltage sufficient to induce ODT breakdown was applied on Probes 1 and 10 for contact sensing. The alignment of the probe array was carefully adjusted such that the output voltages on Probe 1 and 10 dropped to zero almost simultaneously when the probes are lowered. The probe array was then moved through a figure-8 pattern. The writing sequence and the lateral force microscopy (LFM) images of ODT patterns made by probes 2-9 is shown in Figure 15. The fact that all eight DPN tips produce patterns simultaneously indicates that this contact-sensing strategy is effective. The patterns produced by the six probes without gold coating have a line width ranging from 90 to 240nm. However, the two gold-coated probes (Probe 5 and 6) generated much wider lines (650 and 940nm, respectively), possibly due to enlarged tip radius and different surface chemistry conditions. The phenomenon will be investigated more closely in the future.

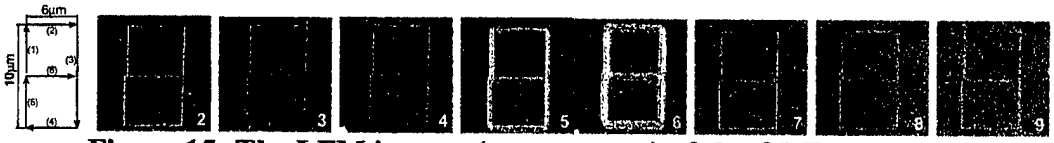

Figure 15: The LFM images (reverse scan) of the ODT patterns.

Area 1.7: We have developed a new method for forming through-wafer microfluidic interconnects. The application of such interconnects is to enable arrayed ink delivery.

A new process for realizing the micropipette array has been proposed and developed (Figure 16). Starting with a silicon wafer, we first perform anisotropic etching (such as deep reactive ion etching) from one or both sides of the silicon wafer. Silicon dioxide is then grown thermally. The oxide film is highly conformal and can grow uniformly even if the sizes of the anisotropically etched openings are small. The silicon oxide on the front side is selectively removed by using mechanical polishing with the cavities temporarily filled with wax (to prevent polishing damages to the interior). Subsequently, we then selectively remove silicon from the front side to a desired depth, revealing silicon oxide tubes with the shell thickness of approximately 1.2 μm.

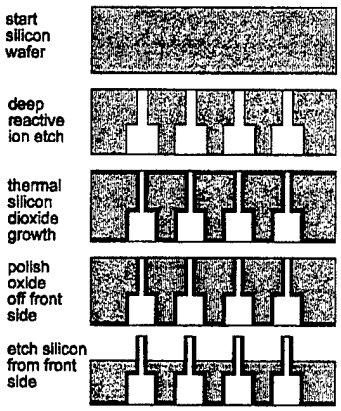

Figure 16: Schematic diagram of fabrication processing of pipette arrays.

This process is simple and offers high yield. Each step of the process flow features high material selectivity and hence robustness in terms of process control. Furthermore, only one layer of thin film growth is needed. One existing method uses LPCVD silicon nitride in conjunction with thermally grown silicon oxide. It involves significantly more materials and process steps. This new method would provide much reduced time and costs.

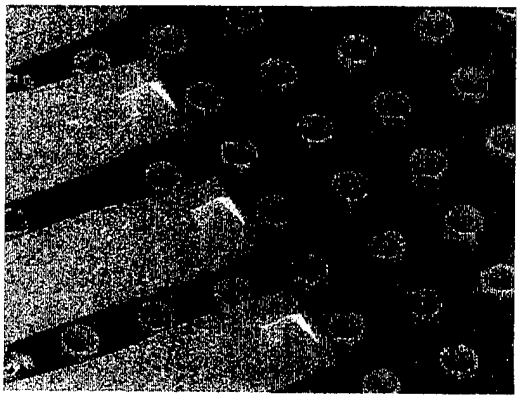

Figure 17: SEM micrograph of pipette array.

Area 1.8: We have developed DPN probes based on low cost polymer materials and a companion fabrication process.

We have developed a new efficient method for creating large arrays of DPN probes with uniform tip geometry, high fabrication yield, and low costs. The fabrication process used a combined surface and bulk micromachining process. Results of a 25x25 array are shown in the figures below (figures 18-20), with incremental levels of magnification.

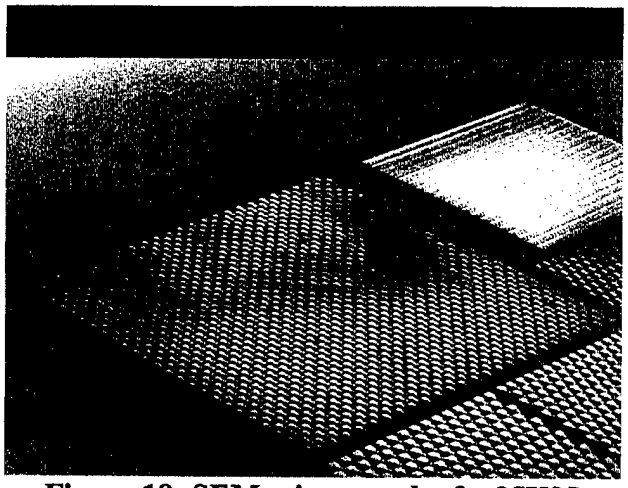

Figure 18: SEM micrograph of a 25X25

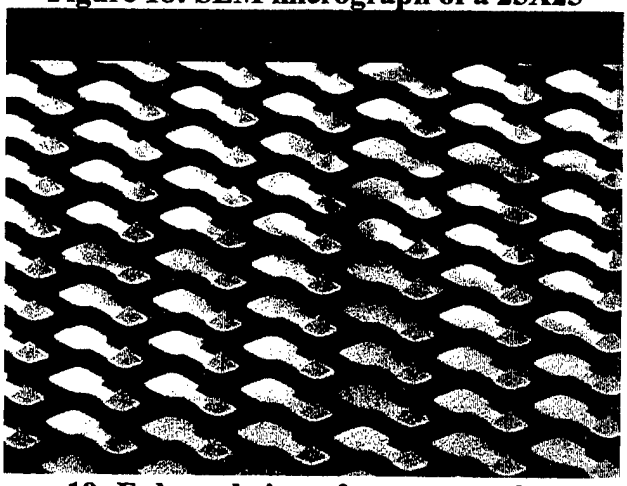

Figure 19: Enlarged view of a segment of an array.

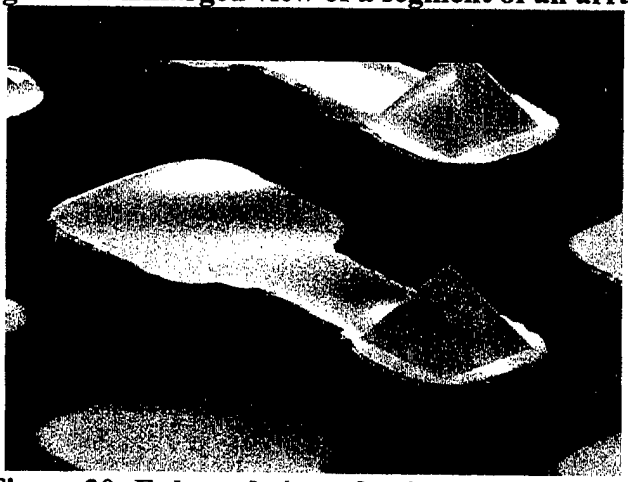

Figure 20: Enlarged view of a single DPN probe.

2. Chemistry developed for the DPN process

The following abstracts are related to the chemistry developed for the DPN process under this award:

Orthogonal Assembly of Nanoparticle Building Blocks on Dip-Pen Nanolithographically Generated Templates of DNA, Demers, L.M.; Mirkin, C. A.; Park, S.-J.; Taton, A.T.; Li, Z. *Angew. Chem. Int. Ed.* **2001**, *40*, 3071-3073.

The development of methods for organizing nanostructures into functional materials with addressable nanoscopic components represents a significant challenge in nanoscience. A variety of methods have been employed to control the assembly of nanoparticles into ordered two- and three-dimensional (2D and 3D) architectures in solution and on surfaces. These involve three general approaches: 1) the use of organic linker molecules and covalent bonding to generate meso- and macroscopic architectures with control over particle placement within an assembled network of particles, 2) the use of external physical forces (e.g. Langmuir techniques, electric fields) and weak interactions to form ordered 2D particle arrays, or 3) the use of biological molecules and their molecular-recognition properties to guide the assembly of polymeric-network structures either on a surface or in solution. However, at present there are no efficient methods for chemically directing the assembly of multicomponent nanostructures on surfaces with precise control over the placement of the nanoscale building blocks. An intriguing possibility for the biomolecule-based approach to particle assembly would be to learn how to pattern biological molecules on surfaces with nanoscale resolution, one could literally chemically program or encode such surfaces with information based upon the biorecognition elements used in the patterning process. For example, in the case of a synthetic sequence of DNA that is 20 bases long, there are 4^{20} possible recognition elements that could be used for guiding the assembly of nanoscale building blocks functionalized with the appropriate complementary sequences. As the length of the sequence increases, the number of recognition elements increases dramatically providing an almost limitless number of interaction pairs that can be designed to guide a given nanostructure-assembly process. In contrast, if ordinary organic molecules were used in either surface-modification chemistry or covalent organic methods for directing such processes, there are a limited and small number of interaction pairs that could be designed and employed. Indeed, Wrighton and co-workers, in studying the assembly of redox-active molecules on micron-scale electrode surfaces made of $In_2 O_3 \pm SnO_2$ (ITO) and Au, respectively, showed that it is difficult to design even two interaction pairs by using coordination chemistry to guide such processes in a perfectly orthogonal manner. We have demonstrated how Dip-Pen Nanolithography (DPN) can be used to create nanostructures of DNA on a surface that can be used subsequently to guide the assembly of discrete nanoparticle building blocks with complementary DNA in an orthogonal manner. Significantly, this strategy could lead to new and general way for preparing multicomponent nanostructures for a wide rang of applications ranging from biological diagnostics to nanoelectronics to the preparation of colloidal crystals for use in catalysis and photonics.

Combinatorial Templates Generated by Dip-Pen Nanolithography for the Formation of Two-Dimensional Particle Arrays, Demers, L. M.; Mirkin, C. A. *Angew. Chem.* **2001**, *40*, 3069-3071.

A general method for organizing micro- and nanoparticles on a substrate could facilitate the formation and study of photonic band-gap arrays for analysis of the relationship between pattern structure and catalytic activity and enable formation of arrays of single protein molecules for proteomics research. While several methods have been reported for assembling collections of particles onto patterned surfaces, a major challenge lies in the selective immobilization of single particles into predetermined positions with respect to adjacent particles. A strategy for chemically and physically immobilizing a wide variety of particle types and sizes with a high degree of control over particle placement calls for a soft lithographic technique capable of high-resolution patterning, as well as one with the ability to form patterns of one or more molecules with precise alignment. Dip-pen nanolithography (DPN) has emerged as one such tool. DPN is a scanning probe nanopatterning technique in which an atomic-force microscopy (AFM) tip is used to deliver molecules to a surface through a water meniscus, which naturally forms in the ambient atmosphere. Significantly, DPN also can be used to generate many customized templates formed from the same or different chemical inks which can be screened under identical conditions for a particular application. We have demonstrated this new combinatorial approach in the context of colloidal crystallization.

Redox-Controlled Orthogonal Assembly of Charged Nanostructures, Ivanisevic, A.; Im, J.H.; Lee, K.B.; Park, S.-J.; Demers, L.M.; Watson, K. J.; Mirkin, C.A. *J. Am. Chem. Soc.* **2001**, *123*, 12424-12425.

Two of the greatest challenges facing researchers working in the areas of nanoscience and nanotechnology are the following: the development of straightforward methods for organizing structures with sub-100 nm dimensions on surfaces into functional architectures and then interfacing such structures with macroscopically addressable components in predefined ways. Although "self-assembly" is often cited as a potential route to addressing these issues, nonliving self-assembled systems lack the hardwired interconnects between their nanoscale components and the macroscopic world. Therefore, it is likely that directed-assembly method, where a predefined pattern guides a desired nanostructure assembly process, rather than self-assembly, will be the first route to device organization on this length scale. One of the emerging strategies for directed-assembly is to use lithographically generated surface templates to guide the assembly of building blocks that recognize such templates through predesigned chemical or physical interactions. Dip-Pen Nanolithography (DPN), electron-beam lithography, and a variety of resist-based scanning probe lithographies have emerged as tools that provide the necessary resolution to create templates that can be used in a directed-assembly processes that involve nanomolar-scale structures. The direct-write nature and soft-matter compatibility of DPN make it particularly attractive for fabricating such templates, especially when they are made from organic molecules. Thus far, it has been demonstrated that DPN-generated templates, comprised of either charged molecules or oligonucleotides, can be used to guide the assembly of particles with complementary charge or oligonucleotide recognition elements, respectively. Herein, we show how one can use redox-active ferrocenylalkyl-thiol "inks" ($Fc(CH_2)_{11}SH$ and $Fc(C{=}O)(CH_{11})SH$),

patterned on a gold substrate, and appropriately applied changes in electrode potential that result in ink oxidation, to trigger and guide the assembly of polyanionic oligonucleotide-modified particles in an orthogonal manner.

"Dip-Pen" Nanolithography on Semiconductor Surfaces, Ivanisevic, A.; Mirkin, C. A. *J. Am. Chem. Soc.* **2001**, *123*, 7887-7889.

Dip-Pen Nanolithography (DPN) uses an AFM tip to deposit organic molecules through a meniscus onto an underlying substrate under ambient conditions. Thus far, the methodology has been developed exclusively for gold using alkyl or aryl thiols as inks. This study describes the first application of DPN to write organic patterns with sub-100 nm dimensions directly onto two different semiconductor surfaces: silicon and gallium arsenide. Using hexamethyldisilazane (HMDS) as the ink in the DPN procedure, we were able to utilize lateral force microscopy (LFM) images to differentiate between oxidized semiconductor surfaces and patterned areas with deposited monolayers of HMDS. The choice of the silazane ink is a critical component of the process since adsorbates such as trichlorosilanes are incompatible with the water meniscus and polymerize during ink deposition. This work provides insight into additional factors, such as temperature and adsorbate reactivity, that control the rate of the DPN process and paves the way for researchers to interface organic and biological structures generated via DPN with electronically important semiconductor substrates.

A MEMS nanoplotter with high-density parallel dip-pen nanolithography probe arrays, Zhang, M.; Bullen, D.; Chung, S.-W.; Hong, S.; Kee, R. S.; Fan, Z.; Mirkin, C.A.; Liu, C. *J. of Nanotechnology* **2002**, *13*, 212-217.

We report on the development of a nanoplotter that consists of an array of microfabricated probes for parallel dip-pen nanolithography. Two types of device have been developed by using microelectromechanical systems micromachining technology. The first consists of 32 silicon nitride cantilevers separated by 100 μm, while the second consists of eight boron-doped silicon tips separated by 310 μm. The former offers writing and imaging capabilities, but is challenged with respect to tip sharpness. The latter offers smaller linewidths and increased imaging capabilities at the expense of probe density. Parallel generation of nanoscopic monolayer patterns with a minimum linewidth of 60 nm has been demonstrated using an eight-pen microfabricated probe array.

Protein Nanoarrays Generated By Dip-Pen Nanolithography, Lee, K.B.; Park, S.-J.; Mirkin, C.A.; Smith, J.C.; Mrksich, M. *Science* **2002**, *295*, 1702-1705.

Dip-pen nanolithography was used to construct arrays of proteins with 100- to 350-nanometer features. These nanoarrays exhibit almost no detectable non-specific binding of proteins to their passivated portions even in complex mixtures of proteins, and therefore provide the opportunity to study a variety of surface-mediated biological recognition processes. For example, reactions involving the protein features and antigens in complex solutions can be screened easily by atomic force microscopy. As further proof-of-concept, these arrays were used to study cellular adhesion at the submicrometer scale.

Moving beyond Molecules: Patterning Solid-State Features via Dip-Pen Nanolithography with Sol-Based Inks, Su, M.; Liu, X.; Li, S.-Y.; Vinayak, D. P.; Mirkin, C.A. *J. Am Chem. Soc.* **2002**, *124,* 1560-1561.

We described a new dip-pen nanolithography (DPN)-based method for the direct patterning of organic/inorganic composite nanostructures on silicon and oxidized silicon substrates. The approach works by the hydrolysis of metal precursors in the meniscus between an AFM tip and a surface according to the reaction $2MCl_n + nH_2O \rightarrow M_2O_n + 2n$HCl; M = Al, Si, and Sn. The inks are hybrid composites of inorganic salts with amphiphilic block copolymer surfactants. Three proof-of-concept systems involving Al_2O_3, SiO_2, and SnO_2 nanostructures on silicon and silicon oxide surfaces have been studied. Arrays of dots and lines can be written easily with control over feature size and shape on the sub-200 nm level. The structures have been characterized by atomic force microscopy, scanning electron microscopy, transmission electron microscopy, and energy-dispersive X-ray analysis. This work is important because it opens up the opportunity for using DPN to deposit solid-state materials rather than simple organic molecules onto surfaces with the resolution of an AFM without the need for a driving force other than chemisorption (e.g., applied fields).

Arrays of Magnetic Nanoparticles Patterned via "Dip-Pen" Nanolithography, Liu, X.; Fu, L.; Hong, S.; Dravid, V.P.; Mirkin, C.A. *Adv. Mat.* **2002**, *14*, 231-234.

There has been considerable recent interest in developing methods for patterning ultrafine magnetic particles because of their potential technological applications in molecular electronics, magnetic storage devices, and biosensors. Advances in nanofabrication technology and lithographic methods have made it possible to: 1) develop new magnetic storage devices with higher storage densities and faster speeds, 2) prepare arrays of interactive magnetic nanoparticles with precisely controlled magnetization orientation and interparticle spacing, and 3) obtain a better understanding of the relationship between magnetic feature size and magnetism. A variety of techniques, including electron-beam lithography, microcontact printing, scanning tunneling microscope lithography, electrochemical etching, and electrodeposition, have been used to fabricate arrays of magnetic structures on semiconductor substrates with dimensions in the sub-100 nm to micrometer length scale. However, there are some inherent limitations associated with these methods including the need for complex instrumentation, costly fabrication procedures, and complex and time-consuming processing steps. Herein, we present a new and straightforward strategy, based upon dip-pen nanolithography (DPN), for preparing nanometer scale magnetic structures with precise feature size control. DPN allows one to transport molecules to a surface, much like a macroscopic dip-pen transfers ink to paper, but with the resolution of a conventional atomic force microscope (AFM), Chemisorption of an ink (e.g., 16-mercaptohexadecanoic acid, MHA) onto the substrate leads to stable nanostructures, which can subsequently be used as templates to assemble different types of molecules or nanostructures of interest, including magnetic nanoparticles and alkylamine-modified deoxyribonucleic acid (DNA).

Direct Patterning of Modified Oligonucleotides on Metals and Insulators by Dip-Pen Nanolithography, Demers, L.M.; Ginger, D.S.; Park, S.-J.; Li, Z.; Chung, S.-W.; Mirkin, C.A. *Science* **2002**, *296,* 1836-1838.

The use of direct-write dip-pen nanolithography (DPN) to generate covalently anchored, nanoscale patterns of oligonucleotides on both metallic and insulating substrates are described. Modification of DNA with hexanethiol groups allowed patterning on gold, and oligonucleotides bearing 59-terminal acrylamide groups could be patterned on derivatized silica. Feature sizes ranging from many micrometers to less than 100 nanometers were achieved, and the resulting patterns exhibited the sequence-specific binding properties of the DNA from which they were composed. The patterns can be used to direct the assembly of individual oligonucleotide-modified particles on a surface, and the deposition of multiple DNA sequences in a single array is demonstrated.

Electrostatically driven Dip-Pen nanolithography of conducting polymers, Lim, J.-H.; Mirkin, C.A. *Adv. Mat.* **2002**, *14*, 1474-1477.

Nanoscale conducting polymer patterns have been fabricated on modified semiconductor substrates using dip-pen nanolithography (DPN). Electrostatic interactions between water-soluble ink materials and charged substrates are the driving force for the generation of stable DPN patterns. The conducting polymers have been characterized by lateral force microscopy and electrochemical methods.

Dip-Pen nanolithography-based methodology for preparing arrays of nanostructures functionalized with oligonucleotides, Zhang, H.; Li, Z.; Mirkin, C.A., *Adv. Mat.* **2002**, *14*, 1472-1473.

Arrays of Au nanostructures have been fabricated based on dip-pen nanolithography and wet chemical etching, where after they can be functionalized with alkanethiol-capped oligonucleotides. These retain their hybridization properties on the surfaces of the nanopatterns and can react with complementary DNA or particles modified with complementary DNA.

Site-directed exchange studies with combinatorial libraries of nanostructures, Ivanisevic, A; McCumber, K.V.; Mirkin, C.A *J. Am. Chem. Soc.* **2002**, *124,* 11997-12001.

We describe a new combinatorial method for studying the exchange between solution adsorbates and nanoscale features within libraries generated via dip-pen nanolithography. Four different compounds, 1-octadecanethiol, 16-mercaptohexadecanoic acid, ferrocene (11-mercaptoundecyl), and ferrocene (11-mercapto-1-oxoundecyl), are studied on amorphous and single-crystal gold substrates. This series of adsorbates allows us to compare the exchange properties of patterns of nanoscale features as a function of composition, feature size, and type of underlying substrate. Moreover, these properties can be compared and contrasted with bulk SAM properties. The novel strategy provides not only a method for initiating site-specific exchange processes but also a way of extracting kinetic information about the rate of such processes in situ.

Fabrication of Sub-50-nm Solid-State Nanostructures on the Basis of Dip-Pen Nanolithography Zhang, H.; Chung, S.-W.; Mirkin, C.A., *Nano Lett.* **2003**, *1*, 43-45.

The fabrication of arrays of sub-50-nm gold dots and line structures with deliberately designed 12-100-nm gaps is reported. These structures were made by initially using dip-pen nanolithography to pattern the etch resist, 16-mercaptohexadecanoic acid, on Au/Ti/Si*O*x/Si substrates and then using wet-chemical etching to remove the exposed gold. Many lithography methods such as electron-beam lithography, photolithography, microcontact printing, nanoimprint lithography, and scanning probe lithography are being used to fabricate structures and patterns on substrates from the micro- to the nanoscale. Very few methods offer the ability to work routinely in the sub-50-nm regime with control over the feature size and interfeature distance, especially when such features are made of both hard and soft materials. Herein we use an experimental method that combines the high-resolution lithographic technique of dip-pen Nanolithography (DPN) with wet-chemical etching to fabricate dot arrays of Au-coated, Ti-coated silicon oxide with features in the 25-50-nm range. In addition, this protocol can be used routinely to make nanogaps ranging from 12 to 100 nm. The novelty in the work presented herein does not lie in the general chemical procedure for using self-assembled mono-layers (SAMs) as wet-chemical etch resists but rather in the scale and geometry (nanogaps) of the structures generated via this approach. Indeed, to the best of our knowledge, these are the smallest Au structures prepared by a wet-chemical etching strategy.

Dip-Pen Nanolithography: What Controls Ink Transport? Rozhok, S.; Piner, R.; Mirkin, C.A. *J. Phys. Chem. B* **2003**, *107*, 751-757.

The influence of temperature and humidity on the growth rates of 1-octadecanethiol (ODT) and 16-mercaptohexadecanoic acid (MHA) monolayers deposited onto a gold substrate has been systematically studied in the context of dip-pen nanolithography (DPN) experiments. By analyzing a statistically meaningful data set, we conclude that for both inks the deposition rate increases with increasing temperature, and that this temperature dependence is strongly affected by relative humidity, chemical nature of the ink and substrate, and writing speed. We attribute these observations to the different solubilities of the ink molecules in water (both the water in the meniscus and on the cantilever walls). In addition, we report a set of experiments that demonstrate meniscus formation even at 0% relative humidity due to residual water that moves to the point of contact between tip and sample.

Electrochemical whittling of organic nanostructures Zhang, Y.; Salaita, K.; Lim, J.-H.; Mirkin, C.A. *Nano Lett.* **2002**, *12*, 1389-1392.

A strategy for reducing the feature size of organic structures on metal surfaces is presented. The approach works by the electrochemical desorption of the peripheries of organic nanostructures (SAMs of 16-mercaptohexadecanoic acid (MHA)) generated by dip-pen nanolithography. By holding the potential of a gold substrate at -750 mV vs Ag/AgCl for designated periods of time in 0.5 M aqueous KOH solution, the size of the MHA nanostructures on the substrate could be reduced in a controlled fashion. It is proposed that the free volume surrounding the nanostructures and the greater ion

accessibility to edge sites facilitate this process. Structures as small as 30 nm could be generated on polycrystalline gold substrates.

Protein Nanostructures Formed via Direct-Write Dip-Pen Nanolithography, Lee, K-B.; Lim, J-H.; Mirkin, C.A. *J. Am. Chem. Soc.* **2003**, in press.

Microarrays of biomolecules such as DNA and proteins have proven useful as high-throughput screening tools in proteomics, genomics, and the identification of new pharmaceutical com-pounds. For example, DNA microarrays can be used to probe gene expression and in panel assays for research- and clinical-based diagnostics. Arrays of proteins have been used to ask and answer important questions regarding the interactions of cells with underlying substrates. As the complexity of these arrays and corresponding number of features increase, the ability to reduce feature size becomes more important, especially since the area occupied by an array will affect the amount and volume of a sample that can be used with a particular chip. Therefore, arrays with smaller and more densely packed features are becoming increasingly attractive. In addition, if one can fabricate such structures with features that have nano- rather than macroscopic dimensions, one can enable new screening technologies and begin to address important fundamental questions regarding biomolecular recognition that are not addressable with microarrays. Indeed, biorecognition is inherently a *nano*- rather than a *micro*scopic phenomenon. Promising advances have been made in making DNA and protein patterns with features with nanoscopic dimensions (<200 nm). However, except in the case of chemically modified collagen and small peptides, protein nanopatterns all have been made by *indirect* methods that either involve resists or prefabricated chemical affinity templates that direct the assembly of a single protein structure from solution onto a set of nanoscopic features on a surface of interest. Note that others have reported the generation of a 600 nm feature of HCG antibody on glass, but the biorecognition properties of this structure and control over feature size on the sub-200 nm scale were not demonstrated.

Direct-Write Dip-Pen Nanolithography of Proteins on Modified Silicon Oxide Surfaces, Lim, J-H.; Ginger, D.S.; Lee, K-B.; Heo, J.; Nam, J-M.; Mirkin, C.A. *Ang. Chem.*, **2003**, *20,* 2411-2414.

The development of direct-write patterning methods for protein-based nanostructures is important for researchers working in the areas of proteomics, diagnostics, and materials science. Such methods could allow one to fabricate patterns of nanostructures of extraordinary complexity, thus offering routes to important tools in the life sciences such as gene chips and proteomic arrays, as well as templates that could be used by chemists and materials scientists to build ordered two-and three-dimensional functional architectures. Although direct-patterning approaches offer many potential advantages over indirect methods (such as facile processing and fabrication procedures, and elimination of the need for resists), they pose several challenges. Methods must be developed for facilitating the transport of the high-molecular-weight biomolecules from a coated tip to a substrate without sacrificing sub-100-nm resolution and patterning speed. Dip-pen nanolithography (DPN) is a promising tool in this respect. However, the area of protein arrays it has thus far been used primarily as a tool for making affinity arrays out of small organic molecules that can subsequently direct the assembly of proteins from

solution. This indirect approach does not allow one to generate arrays made of more than one protein.

Nanopatterning the Chemospecific Immobilization of Cowpea Mosaic Virus Capsid, **Smith, J.C.; Lee, K-B.; Wang, Q.; Finn, M.G.; Johnson, J.E.; Mrksich, M.; Mirkin, C.A.** ***Nano Lett.,*** 2003, Web Release Date: 13-Jun-2003.

This paper presents a novel approach to nanopatterning mixed monolayers using Dip Pen Nanolithography (DPN) for the selective immobilization of bioassemblies. DPN was used with a binary ink consisting of a symmetric 11-mercaptoundecyl-penta (ethylene glycol) disulfide and a mixed disulfide substituted with one maleimide group to pattern nanoscale features that present functional groups for the chemospecific immobilization of cysteine-labeled biomolecules. This strategy was applied to the chemospecific immobilization of cysteine mutant cowpea mosaic virus capsid particles (cys-VCPs). This method will be important for controlling the activities and densities of biological moieties patterned at the nanoscale.

C. Supplementary Information

(1) List of papers submitted, accepted or published:

Demers, L.M.; Mirkin, C. A.; Park, S.-J.; Taton, A.T.; Li, Z. "Orthogonal Assembly of Nanoparticle Building Blocks on Dip-Pen Nanolithographically-Generated Templates of DNA," *Angew. Chem. Int. Ed.* **2001**, *40*, 3071-3073.

Demers, L. M.; Mirkin, C. A. "Combinatorial Templates Generated by Dip Pen Nanolithography for the Formation of Two-Dimensional Particle Arrays," *Angew. Chem.* **2001**, *40*, 3069-3071.

Ivanisevic, A.; Im, J.H.; Lee, K.B.; Park, S.-J.; Demers, L.M.; Watson, K. J.; Mirkin, C.A. "Redox-Controlled Orthogonal Assembly of Charged Nanostructures," *J. Am. Chem. Soc.* **2001**, *123*, 12424-12425.

Ivanisevic, A.; Mirkin, C. A."'Dip-Pen' Nanolithography on Semiconductor Surfaces," *J. Am. Chem. Soc.* **2001**, *123*, 7887-7889.

Zhang, M.; Bullen, D.; Chung, S.-W.; Hong, S.; Kee, R. S.; Fan, Z.; Mirkin, C.A.; Liu, C. "A MEMS Nanoplotter with High-Density Parallel Dip Pen Nanolithography (DPN) Probe Arrays," *J. of Nanotechnology* **2002**, *13*, 212-217.

Lee, K.B.; Park, S.-J.; Mirkin, C.A.; Smith, J.C.; Mrksich, M. "Protein Nanoarrays Generated By Dip-Pen Nanolithography," *Science* **2002**, *295*, 1702-1705.

Su, M.; Liu, X.; Li, S.-Y.; Vinayak, D. P.; Mirkin, C.A. "Moving Beyond Molecules: Patterning Solid State Features via Dip-Pen Nanolithography With Sol-based Inks," *J. Am Chem. Soc.* **2002**, *124,* 1560-1561.

Liu, X.; Fu, L.; Hong, S.; Dravid, V.P.; Mirkin, C.A. "Arrays of Magnetic Nanoparticles via "Dip Pen" Nanolithography," *Adv. Mat.* **2002**, *14*, 231-234.

Demers, L.M.; Ginger, D.S.; Park, S.-J.; Li, Z.; Chung, S.-W.; Mirkin, C.A. "Direct Patterning of Modified Oligonucleotides on Metals and Insulators via Dip-Pen Nanolithography," *Science* **2002**, *296,* 1836-1838.

Lim, J. -H.; Mirkin, C.A. "Electrostatically Driven Dip-Pen Nanolithography of Conducting Polymers," *Adv. Mat.* **2002**, *14*, 1474-1477.

Zhang, H.; Li, Z.; Mirkin, C.A. "Dip-Pen Nanolithography-Based Methodology for Preparing Arrays of Nanostructures Functionalized with Oligonucleotides," *Adv. Mat.* **2002**, *14*, 1472-1473.

Ivanisevic, A; McCumber, K.V.; Mirkin, C.A "Site -Directed Exchange Studies With Combinatorial Libraries of Nanostructures," *J. Am. Chem. Soc.* **2002**, *124,* 11997-12001.

Zhang, H.; Chung, S.-W.; Mirkin, C.A. "Fabrication of sub-50 nm Solid-State Nanostructures Based on Dip-Pen Nanolithography," *Nano Lett.* **2003**, *1*, 43-45.

Rozhok, S.; Piner, R.; Mirkin, C.A. "Dip-Pen Nanolithography: What Controls Ink Transport?" *J. Phys. Chem. B* **2003,** *107*, 751-757.

Zhang, Y.; Salaita, K.; Lim, J.-H.; Mirkin, C.A. "Electrochemical Whittling of Organic Nanostructures," *Nano Lett.* **2002**, *12*, 1389-1392.

Lee, K-B.; Lim, J-H.; Mirkin, C.A. "Protein Nanostructures Formed Via Direct-Write Dip-Pen Nanolithography" *J. Am. Chem. Soc.* **2003**, in press.

Lim, J-H.; Ginger, D.S.; Lee, K-B.; Heo, J.; Nam, J-M.; Mirkin, C.A. "Direct-Write Dip-Pen Nanolithography of Proteins on Modified Silicon Oxide Surfaces," *Ang. Chem.,* **2003,** *20,* 2411-2414.

Smith, J.C.; Lee, K-B.; Wang, Q.; Finn, M.G.; Johnson, J.E.; Mrksich, M.; Mirkin, C.A.; "Nanopatterning the Chemospecific Immobilization of Cowpea Mosaic Virus Capsid" *Nano Lett.,* **2003,** Web Release Date: 13-Jun-2003.

(2) Scientific Personnel

Post Doctoral Associates:
Dr. Sung Wook Chung/NU
Dr. Jung-Hyurk Lim/NU
Dr. Sergey Rozhok/NU
Dr. Hua Zhang/NU
Dr. Yi Zhang/NU
Dr. Jun Zhou/U of I

Graduate Students:
Ki-Bum Lee/NU
Khalid Salaita/NU
David Bullen/U of I
Xuefeng Wang/U of I

Both Linette Demers and So-Jung Park form Northwestern University are PhD recipients while employed on this project.

(3) Report of Inventions

NU 22008: "Patterning Solid-State Features Via Dip-Pen Nanolithography with Sol-Based Inks"

a) Provisional Application 60/341,614 filed 12/17/01
b) U. S. Application 10/320,721 filed 12/17/02PCT/US02/40118 filed 12/17/02 Filed in Taiwan 12/16/02
c) Inventors: Chad Mirkin, Vinayak Dravid, Ming Su

NU 22058: "Electrochemical Whittling of Lithographically Defined Structures"

a) Provisional Application 60/394,141 filed 7/5/02 Filed 7/5/02
b) Inventors: Chad Mirkin, Yi Zhang, Khalid Salaita

NU 22077: "Nanopatterning of "Hard" Magnetic Nanostructures Via Dip-Pen Nanolithography and a Sol-Based Ink"

a) Provisional Application filed 9/17/02 as 60/410,952
b) Inventors: Lei Fu, Xiaogang Liu, Vinayak Dravid, Chad Mirkin

NU 22116: "Protein Arrays with Nanoscopic Features Generated by Dip-Pen Nanolithography"

a) Provisional Patent Application 60/326,767 filed 10/2/01
b) U. S. Patent Application 10/261,663 filed 10/2/02PCT/US02/31214 filed 10/2/02 Filed in Taiwan 10/2/02
c) Inventors: Chad Mirkin, So-Jung Park, Ki-Bum Lee

NU 22117: "Fabrication of sub-50nm Solid State Nanostructures Based on Dip-Pen Nanolithography"

a) Provisional application filed 12/3/02 – 60/430,349
b) Inventors: Chad Mirkin Hua Zhang, Sung-Wook Chung

NU 23038: "Peptide and Protein Nanoarrays and Direct-Write Nanolithographic Printing of Peptides and Proteins"

a) Provisional Application 60/60/418,179 filed 10/15/02PCT filed 5/21/03 – Us filed in PCT – combined with NU 23040
b) Inventors: Chad Mirkin, Jung-Hyurk Lim, David Ginger, Ki-Bum Lee, Jwa-Min Nam, Linette Demers

NU 23039: "Nanoparticle Assemblies"

a) Provisional Application 60/434,248 filed 12/17/02
b) Inventors: Chad Mirkin, Rongchao Jin, Li Zhi

NU 23040: "Peptide and Protein Nanoarrays and Direct-Write Nanolothographic Printing of Peptides and Proteins"

a) Provisional Application 60/445,233 filed 2/6/03PCT filed 5/21/03 – US in PCT combined with NU 23038
b) Inventors: Chad Mirkin, Jung-Hyurk Lim, David Ginger, Ki-Bum Lee, Jwa-Min Nam, Linette Demers

NU 23045: "Electrochemical Whittling of Lithographically Defined Structures"

a) Being combined with 22058 -- application in preparation
b) Inventors: Chad Mirkin, Yi Zhang, Khalid Salaita

TF03002: "A Hybrid Microfluid Chip Architecture and the Fabrication Process for Such"

a) **Actively Manage** (Med-High);
b) Provisional Patent Protection by 6/4/03 will merge with TF02036 into Regular US Utility Appl., discussed with Fallon/Ranson/Liu on 5/20/03;
c) Inventors: Chang Liu, Shaikh, Ryu.

TF01031: "Nanoscale Chemical Surface Patterning Dip Pens"

a) **License Negotiation** (Med-High) **Assessed**; primary licensing interest will be NanoInk, Inc.;
b) US Patent Application 10/008,719, filed on 12/7/01, "Parallel, Individually Addressable Probes for Nanolithography" (Some claims in condition for allowance response filed 5/8/03);
c) Inventors: Chang Liu, Zhang, David Bullen;

TF02040: "A Method of Dispensing Fluids Using Microfabricated Micro Pipette Array and The Fabrication Process of Such Arrays"

a) **License Negotiation** (Med-High) **Assessed**; primary licensing interest will be NanoInk, Inc.;
b) US Patent Application in draft (Rauch);
c) Inventors: Chang Liu, Ryu, David Bullen;

TF02082: "An Efficient Method To Make Scanning Probe Microscopy (SPM) Probes with Sharp Tips"

a) **License Negotiation** (Med-High), primary licensing interest will be NanoInk, Inc.;
b) US Patent Application in draft, initial application is joint with Northwestern Univ. (Mirkin) then individual institution continuations (Rauch);
c) Inventors: Liu, Zou, Wang, David Bullen; Chad A. Mirkin